Biochemical Pharmacology 78 (2009) 1464–1474

Contents lists available at ScienceDirect

Biochemical Pharmacology

journal homepage: www.elsevier.com/locate/biochempharm

Monocomponent hexa- and dodecaethylene glycol succinyl-tocopherol esters: Self-assembly structures, cellular uptake and sensitivity to enzyme hydrolysis

Britta M. Folmer [a,1], Denis Barron [a], Eric Hughes [a], Laurence Miguet [a], Belén Sanchez [a], Olivier Heudi [a], Martine Rouvet [a], Laurent Sagalowicz [a], Philippe Callier [a], Martin Michel [a], Gary Williamson [a,b,*]

[a] Nestlé Research Center, Vers-chez-les-Blanc, 1000 Lausanne 26, Switzerland
[b] School of Food Science and Nutrition, University of Leeds, Leeds, LS2 9JT, UK

ARTICLE INFO

Article history:
Received 20 May 2009
Accepted 16 July 2009

Keywords:
Self-assembly structure
Esterase
Caco-2 cell
Docking model
Vitamin E

ABSTRACT

We have chemically synthesized two water-soluble forms of tocopherol succinate linked via an ester bond to hexaethylene glycol and dodecaethylene glycol. The self-assembly structure of the former in water is vesicular, whereas the latter forms elongated micelles. We treated Caco-2 cells with these compounds in these physical forms, in addition to a mixed micelle form. The intact compounds were taken up into the cells, influenced by both the chain length and the physical structure. In addition, the tocopherol derivatives were also metabolized into tocopherol succinate and tocopherol inside the cell. The total hydrolysis and uptake into the cells was two-fold higher from tocopherol hexaethylene glycol succinate in the form of mixed micelles than in vesicular form as assessed by analyzing intracellular tocopherol and tocopherol succinate. The longer polyethylene glycol chain gave a higher intracellular tocopherol succinate/tocopherol ratio. The major intracellular esterase in Caco-2 cells is carboxyl esterase 1 (EC 3.1.1.1), and in silico modelling studies show that the position of docking and hence the site of hydrolysis is influenced by the chain length. The in silico prediction is consistent with the in vitro data, since a longer chain length is predicted to favour hydrolysis of the ester bond between the succinate and polyethylene glycol moieties.

1. Introduction

α-Tocopherol (vitamin E, cpd 1; Fig. 1) has numerous biological properties [1–3]. In low fat conditions such as maldigestion or enteral feeding, the bioavailability of tocopherol in the gut is compromised, which has led to the proposal for water-soluble forms of tocopherol to be used under these conditions. α-Tocopherol succinate (cpd 2) and acetate (cpd 3) serve as such dietary sources of (cpd 1) upon de-esterification. The succinate ester, but not the acetate, demonstrates biological activity such as antiproliferative activity, induction of cell apoptosis and regulation of cell differentiation. The different biological activities of these forms of α-tocopherol are related to their interactions with membrane phospholipids and membrane associated proteins [4,5].

Various interfacially active derivatives of tocopherol have been described in the literature such as α-tocopherol polyethylene glycol succinate 1000 (TPGS) (cpd 4), which is synthesized by reaction of the tocopherol succinate with ethylene oxide, leading to a dispersity in the polyethylene oxide chain, with an average of ca. 23 units. (Cpd 4) has been proposed both for increased delivery and bioavailability of (cpd 1), but also as an emulsifier and delivery system for lipophilic molecules. In the latter case, TPGS has been suggested as a drug solubilising agent and to enhance drug functionality [5,6].

Although proposed as a delivery system for (cpd 1), whether hydrolysis of the polyethylene glycol moiety of (cpd 4) occurs before absorption is controversial. For the dietary supplementation by (cpd 4) of one patient having short-bowel syndrome, supplementation with (cpd 3) did not increase the uptake of (cpd 1), whereas (cpd 4) increased (cpd 1) in plasma to normal levels [6]. In a feeding experiment with broiler chickens, (cpd 1) and (cpd 3) were absorbed normally whereas (cpd 4) was poorly absorbed, due to the low affinity of esterases for (cpd 4) in the intestine of broiler chickens [7].

Various other derivatives of α-tocopherol and their bioavailability in healthy subjects have been described in the literature. The aminoalkanecarboxylic acid ester of α-tocopherol is an

Abbreviations: cpd, compound; cryo-TEM, cryogenic transmission electron microscopy; EDCI, *N*-(3-dimethylaminopropyl)-*N'*-ethylcarbodiimide hydrochloride; hCE1, human carboxyl esterase 1 enzyme; MM, mixed micellar form; THF, tetrahydrofuran; TPGS, α-tocopherol polyethylene glycol succinate 1000; VLC, vacuum liquid chromatography.

* Corresponding author at: Nestlé Research Center, Vers-chez-les-Blanc, 1000 Lausanne 26, Switzerland. Tel.: +41 21 785 8546; fax: +41 21 785 8544.
E-mail address: gary.williamson@rdls.nestle.com (G. Williamson).
[1] Current address: Nestlé Nespresso, Rte du Lac 3, CH 1094, Paudex, Switzerland.

0006-2952/$ – see front matter © 2009 Elsevier Inc. All rights reserved.
doi:10.1016/j.bcp.2009.07.009

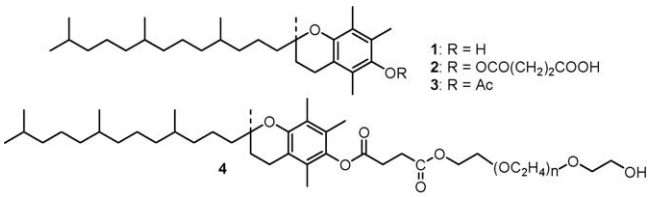

Fig. 1. The structure of tocopherol and derivatives: (cpd 1) α-tocopherol; (cpd 2) α-tocopherol succinate; (cpd 3) α-tocopherol acetate; (cpd 4) α-tocopherol polyethylene glycol succinate 1000 (TPGS).

ionically charged and water-soluble molecule that is expected to be hydrolyzed in the intestine [8,9]. A tocopherol hydrogel for biomedical applications was obtained by copolymerization of tocopherol-methacrylate with 2-hydroxyethyl methacrylate [10], and 5 α-tocopheryl ascorbate has been synthesized [11–13].

In the present study, two defined derivatives of TPGS are used as a model system to study the bioavailability of (cpd 1) as a function of its hydrophilic–lipophilic balance, e.g. its solubility in water, oil or at the interface. α-Tocopherol succinates with monodisperse polyethylene glycol chains were synthesized for the first time. The lengths of the hydrophilic chains were 6 and 12 ethylene oxide units (tocopherol hexaethylene glycol succinate (cpd 9) and tocopherol dodecaethylene glycol succinate (cpd 13), respectively). We hypothesized that the interfacial activity as well as the self-assembly structure of the compounds would influence the rate of enzymatic hydrolysis. Absorption studies were carried out using Caco-2 cells, a human intestinal cell line derived from a carcinoma of the colon, which has certain characteristics of mature enterocytes. The absorption of the vitamin derivatives by the cells was studied and the influence of the polyethylene glycol chain length on aggregate formation was assessed by NMR self-diffusion and cryogenic transmission electron microscopy (cryo-TEM). The effect of the aggregate shape on the bioavailability of the compound in Caco-2 cells was also examined. Structure-based molecular docking calculations using a three-dimensional structure of the human carboxyl esterase 1 were performed to give insight into the hydrolytic mechanism of the tocopherol polyethylene glycol succinate molecules for delivering tocopherol, and to analyze the hydrolysis as a function of polyethylene glycol chain length. A data set containing 20 different tocopherol derivatives was designed and screened, and the virtual docking calculations allowed determination of the optimal chain length for hydrolysis.

2. Materials and methods

2.1. Materials

Hexaethylene glycol and $CDCl_3$ (99.8% deuterium) was from Aldrich, Buchs, Switzerland. Butyl hydroxytoluene, benzyl bromide and *N*-(3-dimethylaminopropyl)-*N*′-ethylcarbodiimide hydrochloride (EDCI) were obtained from Fluka, Buchs, Switzerland; 5% Pd on carbon was from Acros Organics, Geel, Belgium. Cells used were Caco-2 HTB37 between passages 24 and 28. Thin layer chromatography was carried out on Merck Silica 60 F254, RP-18 F254s, or DIOL F254s plates (VWR International, Nyon, Switzerland). Vacuum liquid chromatography was performed on silica gel 60 (63–200 μM), or on a bonded phase-octadecyl (C18) for flash chromatography (40 μM average particle diameter). ^{1}H NMR (300.13 MHz) and ^{13}C NMR (90.56 MHz) spectra were recorded on a Bruker DPX-360 apparatus, equipped with a 5 mm BBO gradient head, and using $CDCl_3$ as solvent. Foetal bovine serum, non-essential amino acids, gentamicin and fungizon were from Invitrogen, Basel, Switzerland. α-Tocopherol succinate (cpd 2), Dulbecco's modified Eagle's medium containing 4.5 g glucose/L, penicillin, streptomycin, monoolein, lysophosphatidylcholine, oleic acid and taurocholic acid were all from Sigma, Basel, Switzerland.

2.2. Synthetic procedures

Hexaethylene glycol monobenzyl ether (cpd 7) (*see* Scheme 1): a mixture of 20 mL (79.83 mmol) of hexaethylene glycol (cpd 5), 6 mL (60 mmol) of 40% aq. NaOH, and 2.4 mL (20.2 mmol) of benzyl bromide (cpd 6) was stirred at 100 °C (oil bath) under stirring for 24 h. After cooling the medium was diluted with 20 mL of a satd. aq. NaCl solution, and extracted by 4 × 200 mL of EtOAc. The EtOAc extract was dried over anhydrous sodium sulfate and concentrated under reduced pressure. Purification of the residue by VLC on RP-18, using a gradient of MeOH in H_2O as solvent, afforded 5.4 g (14.5 mmol; 72%) of compound (cpd 7) [14–18] as a colourless oil. Silica hexane-EtOAc 6/4, R_f = 0.21; RP-18 MeOH-H_2O 6/4, R_f = 0.41 (tailing); diol hexane-iPrOH 8/2, R_f = 0.21 (tailing). ^{1}H

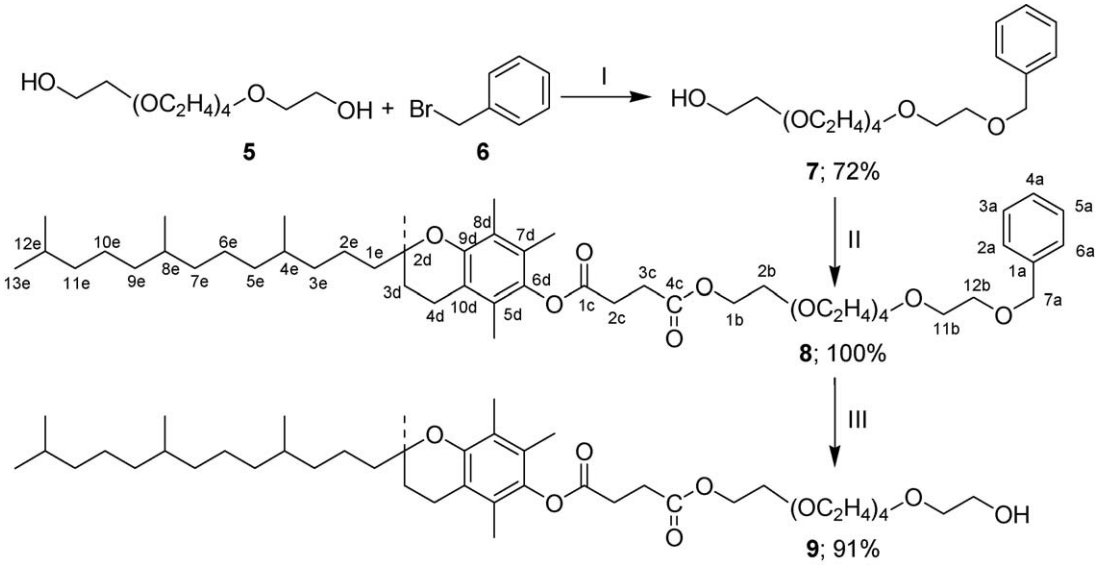

Scheme 1. The preparation of α-tocopherol hexaethylene glycol succinate (cpd 9). (I) Aq. NaOH, 100 °C, 24 h; (II) tocopherol succinate (cpd 2), EDCI, 16 h, 25 °C; (III) H_2, 5% Pd/C, 1 bar, 25 °C, 3 h.

NMR ($CDCl_3$) δ 3.61–3.68 (m, 24H, H1b–12b), 4.56 (s, 2H, H7a), 7.24–7.36 (m, 5H, H2a–6a). ^{13}C NMR ($CDCl_3$) δ 61.63 (C1b), 69.39 (C12b), 70.25 (C2b), 70.49, 70.51, 70.55, 70.57, 70.60 and 72.59 (C3b–C11b), 73.19 (C7a), 127.56 (C4a), 127.72 (C2a/6a), 128.33 (C3a/5a), 138.24 (C1a).

α-Tocopherol succinyl benzylhexaethylene glycol (cpd 8): 1 g (2.68 mmol) of hexaethylene glycol monobenzyl ether (cpd 7) was dissolved in 20 mL of CH_2Cl_2. 1.5 g (2.83 mmol) of (+)-α-tocopherol succinate (cpd 2), 130 mg (1.06 mmol) of dimethylaminopyridine, and 1.6 g (8.35 mmol) of EDCI were added, successively, under stirring. The medium was allowed to react at 22 °C under stirring for 16 h. The medium was directly purified by VLC on silica using a gradient of Me_2CO in hexane as solvent, to give 2.37 g (2.68 mmol; 100%) of α-tocopherol succinyl benzylhexaethylene glycol (cpd 8) as a colourless oil. Silica hexane-EtOAc 6/4, R_f = 0.49. ^1H NMR ($CDCl_3$) δ 0.84 (d, J = 6.6 Hz, 3H, 4eMe[a]), 0.85 (d, J = 6.5 Hz, 3H, 8eMe[a]), 0.86 (d, J = 6.6 Hz, 6H, H13e + 12eMe), 1.00–1.60 (m, 21H, H1e–12e), 1.23 (s, 3H, 2dMe), 1.77 (m, 2H, H3d), 1.97 (s, 3H, 5dMe), 2.01 (s, 3H, 7dMe), 2.08 (s, 3H, 8dMe), 2.58 (brt, J = 6.7 Hz, 2H, H4d), 2.79 (brt, J = 6.9 Hz, 2H, H3c), 2.93 (m, 2H, H2c), 3.61–3.71 (m, 22H, H2b–12b), 4.26 (brt, J = 4.8 Hz, 2H, H1b), 4.56 (s, 2H, H7a), 7.24–7.36 (m, 5H, H2a–6a). ^{13}C NMR ($CDCl_3$) δ 11.81 (8dMe), 12.09 (5dMe), 12.94 (7dMe), 19.65 (8eMe[a]), 19.75 (4eMe[a]), 20.58 (C4d), 21.01 (C2e), 22.63 (C13e[b]), 22.73 (12eMe[b]), 23.78–24.00 (br signal, 2dMe), 24.43 (C6e), 24.79 (C10e), 27.97 (C12e), 28.81 (C2c), 29.08 (C3c), 31.08 (br signal, C3d), 32.70 (C4ec), 32.78 (C8ec), 37.27 (C3e), 37.41 and 37.44 (C5e + C7e + C9e), 39.36 (C11e), 39.77–40.33 (br signal, C1e), 63.92 (C1b), 69.05 (C2b), 69.42 (C12b), 70.55, 70.58, 70.59 and 70.64 (C3b–C11b), 73.22 (C7a), 75.03 (C2d), 117.35 (C10d), 122.99 (C7d), 124.93 (C5d), 126.67 (C8d), 127.57 (C4a), 127.73 (C2a/6a), 128.35 (C3a/5a), 138.26 (C1a), 140.42 (C6d), 149.40 (C9d), 170.93 (C1c), 172.18 (C4c).

α-Tocopherol succinyl hexaethylene glycol (cpd 9): 890.6 mg (1 mmol) of α-tocopherol succinyl benzylhexaethylene glycol (cpd 8) was dissolved in a mixture of 5 mL of hexane and 5 mL of EtOH. 100 mg of 5% Pd/C was added and the medium allowed reacting at 22 °C under H_2 atmosphere, at atmospheric pressure with stirring for 3 h. The catalyst was removed by filtration and washed with 2 × 5 mL of EtOH. The filtrate and the two washings were concentrated under reduced pressure and dried to give 723 mg (0.91 mmol; 91%) of compound (cpd 9) as a colourless oil. Diol hexane-iPrOH 8/2, R_f = 0.33. ^1H NMR ($CDCl_3$) δ 0.84 (d, J = 6.6 Hz, 3H, 4eMe[a]), 0.85 (d, J = 6.5 Hz, 3H, 8eMe[a]), 0.87 (d, J = 6.7 Hz, 6H, H13e + 12eMe), 1.09 (m, 2H, H3e), 1.14 (m, 2H, H11e), 1.23 (s, 3H, 2dMe), 1.20–1.30 (m, 6H, H5e + H7e + H9e), 1.38 (m, 2H, H4e + H8e), 1.52 (m, 1H, H12e), 1.77 (m, 2H, H3d), 1.97 (s, 3H, 5dMe), 2.01 (s, 3H, 7dMe), 2.09 (s, 3H, 8dMe), 2.58 (brt, J = 6.7 Hz, 2H, H4d), 2.79 (brt, J = 6.9 Hz, 2H, H3c), 2.93 (m, 2H, H2c), 3.59–3.73 (m, 22H, H2b–12b), 4.27 (brt, J = 4.8 Hz, 2H, H1b). ^{13}C NMR ($CDCl_3$) δ 11.81 (8dMe), 12.06 (5dMe), 12.93 (7dMe), 19.66 (8eMe[a]), 19.75 (4eMe[a]), 20.58 (C4d), 21.01 (C2e), 22.63 (C13e[b]), 22.73 (12eMe[b]), 23.43–24.29 (br signal, 2dMe), 24.44 (C6e), 24.80 (C10e), 27.97 (C12e), 28.82 (C2c), 29.08 (C3c), 31.08 (br signal, C3d), 32.70 (C4e[c]), 32.78 (C8e[c]), 37.27, 37.41 and 37.44 (C3e + C5e + C7e + C9e), 39.36 (C11e), 39.57–40.42 (br signal, C1e), 61.70 (C12b), 63.94 (C1b), 69.06 (C2b), 70.28, 70.52, 70.55, 70.60 and 72.59 (C3b–C11b), 75.04 (C2d), 117.36 (C10d), 122.99 (C7d), 124.93 (C5d), 126.67 (C8d), 140.43 (C6d), 149.40 (C9d), 170.95 (C1c), 172.21 (C4c). Analysis: calcd. for $C_{45}H_{78}O_{11}$ $0.3CH_2Cl_2$: C, 66.31; H, 9.65. Found: C, 66.55; H, 9.68.

Mono-O-benzylhexaethylene glycol tosylate (cpd 10) (*see* Scheme 2): 1.41 g (3.79 mmol) of monobenzyl hexaethylene glycol (cpd 7) was dissolved in 20 mL of CH_2Cl_2. 2.5 mL (18.03 mmol) of triethylamine, and 0.87 g (4.56 mmol) of toluene 4-sulfonyl chloride were added successively, under stirring at RT. The reaction was allowed to take place at 22 °C under stirring for 14 h. The medium was diluted with 20 mL of CH_2Cl_2. The CH_2Cl_2 extract was washed with 50 mL of 1N aq. HCl and 3 × 50 mL of H_2O. The CH_2Cl_2 was evaporated under reduced pressure and the residue was dried in a dessicator (oil pump) for 6 h, to give 1.33 g (2.52 mmol; 66%) of compound (cpd 10) [15,17] as a colourless oil. Silica EtOAc, R_f = 0.52 (tailing). ^1H NMR ($CDCl_3$) δ 2.44 (s, 3H, H7c), 3.57–3.70 (m, 22H, H2b–12b), 4.15 (brt, J = 4.7 Hz, 2H, H1b), 4.56 (s, 2H, H7a), 7.24–7.34 (m, 7H, H3c/5c and H2a–6a), 7.80 (d, J = 8.5 Hz, 2H, H2c/6c). ^{13}C NMR ($CDCl_3$) δ 21.66 (C7c), 68.25 (C2b), 69.23 (C1b), 69.42 (C12b), 70.50, 70.54, 70.56, 70.58, 70.59, 70.63 and 72.72 (C3b to C11b), 73.21 (C7a), 127.58 (C4a), 127.72 (C2a/6a), 127.97 (C2c/6c), 128.35 (C3a/5a), 129.81 (C3c/5c), 132.99 (C1c), 138.26 (C1a), 144.79 (C4c).

Dodecaethylene glycol monobenzyl ether (cpd 11): 0.6 g (15 mmol; 1 eq.) of a 60% dispersion of sodium hydride was added to a solution of 4 g (14.16 mmol) of hexaethylene glycol (cpd 5) in 25 mL of dry THF. The mixture was refluxed (oil bath 90 °C) under stirring for 10 min. After cooling of the medium, a solution of 1.33 g (2.52 mmol) of tosyl benzylhexaethylene glycol (cpd 10) in 25 mL of dry THF was added. The mixture was refluxed (oil bath 90 °C) under stirring for 30 min. The solvent was evaporated under reduced pressure. The residue was cooled in an ice bath and acidified by addition of 15 mL of ice cold 1N aq. HCl. 2 mL of MeOH were added to complete the dissolution of the residue. The medium was directly purified by VLC on RP-18 using a gradient of

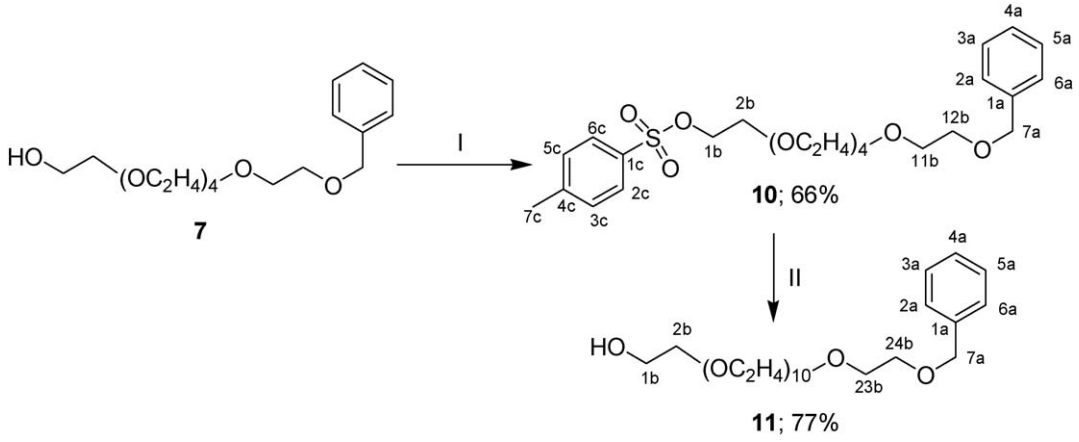

Scheme 2. The preparation of dodecaethylene glycol monobenzyl ether (cpd 11). (I) Toluene 4-sulfonyl chloride, triethylamine, 14 h, 25 °C; (II) excess hexaethylene glycol, NaOH, 90 °C, 10 and 30 min.

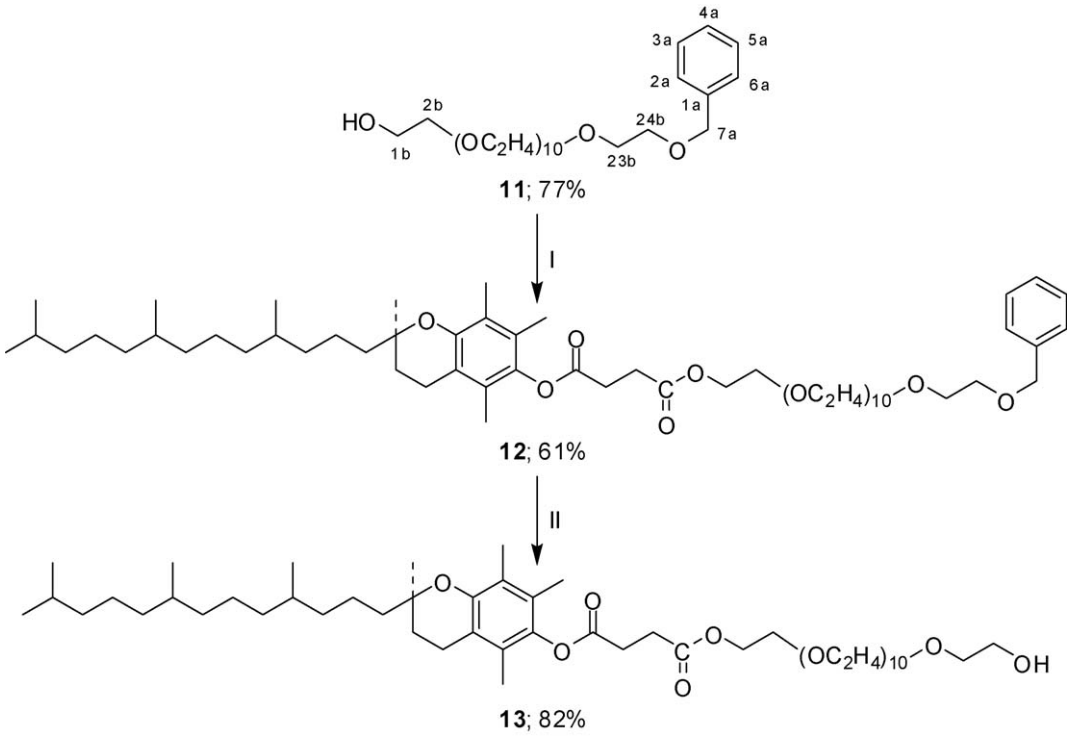

Scheme 3. The preparation of α-tocopherol dodecaethylene glycol succinate (cpd 13). (I) α-Tocopherol succinate (cpd 2), EDCI, 16 h, 25 °C; (II) H_2, 5% Pd/C, 1 bar, 22 °C, 3 h.

MeOH in H_2O as solvent. This yielded 1.23 g (1.93 mmol; 77%) of compound (cpd 11) as a colourless oil. RP-18 MeOH-H_2O 7/3, R_f = 0.46 (tailing).

α-Tocopherol succinyl benzyldodecaethylene glycol (cpd 12) (*see* Scheme 3): 530 mg (0.83 mmol) of dodecaethylene glycol monobenzyl ether (cpd 11) was dissolved in 5 mL of CH_2Cl_2. 440 mg (0.83 mmol) of (+)-α-tocopherol succinate (cpd 2), 40 mg (0.33 mmol) of dimethylaminopyridine (DMAP), and 500 mg (2.61 mmol) of EDCI were added, successively, under stirring. The medium was allowed to react at 22 °C under stirring for 16 h. The medium was diluted with 20 mL of CH_2Cl_2 and directly purified by VLC on silica, using a gradient of Me_2CO in CH_2Cl_2 as solvent. This afforded 581 mg (0.51 mmol; 61%) of (cpd 12) as a colourless oil. Silica CH_2Cl_2-Me_2CO 6/4, R_f = 0.56. ^{1}H NMR ($CDCl_3$) δ 0.84 (d, J = 6.6 Hz, 3H, 4eMe^a), 0.85 (d, J = 6.5 Hz, 3H, 8eMe^a), 0.86 (d, J = 6.6 Hz, 6H, H13e + 12eMe), 1.00–1.60 (m, 21H, H1e–12e), 1.23 (s, 3H, 2dMe), 1.77 (m, 2H, H3d), 1.97 (s, 3H, 5dMe), 2.01 (s, 3H, 7dMe), 2.08 (s, 3H, 8dMe), 2.58 (brt, J = 6.7 Hz, 2H, H4d), 2.79 (brt, J = 6.8 Hz, 2H, H3c), 2.93 (brt, J = 6.8 Hz, 2H, H2c), 3.63–3.71 (m, 46H, H2b–24b), 4.27 (brt, J = 4.8 Hz, 2H, H1b), 4.56 (s, 2H, H7a), 7.24–7.36 (m, 5H, H2a–6a). ^{13}C NMR ($CDCl_3$) δ 11.81 (8dMe), 12.09 (5dMe), 12.93 (7dMe), 19.66 (8eMe^a), 19.75 (4eMe^a), 20.58 (C4d), 21.00 (C2e), 22.63 (C13e^b), 22.73 (12eMe^b), 23.57–24.24 (br signal, 2dMe), 24.43 (C6e), 24.79 (C10e), 27.96 (C12e), 28.81 (C2c), 29.07 (C3c), 31.08 (br signal, C3d), 32.69 (C4e^c), 32.77 (C8e^c), 37.26, 37.40 and 37.43 (C3e, C5e + C7e + C9e), 39.36 (C11e), 39.62–40.49 (br signal, C1e), 63.91 (C1b), 69.05 (C2b), 69.41 (C24b), 70.55 and 70.63 (C3b to C23b), 73.22 (C7a), 75.03 (C2d), 117.35 (C10d), 122.99 (C7d), 124.93 (C5d), 126.67 (C8d), 127.58 (C4a), 127.73 (C2a/6a), 128.34 (C3a/5a), 138.25 (C1a), 140.42 (C6d), 149.40 (C9d), 170.94 (C1c), 172.19 (C4c).

α-Tocopherol succinyl dodecaethylene glycol (cpd 13): 389.3 mg (0.34 mmol) of α-tocopherol succinyl benzyldodecaethylene glycol (cpd 12) was dissolved in a mixture of 2 mL of EtOH and 2 mL of hexane. 50 mg of 5% Pd/C was added and the medium was allowed to react at 22 °C under H_2 atmosphere, at atmospheric pressure with stirring for 3 h. The catalyst was removed by filtration and washed with 3 × 1.5 mL of EtOH. The filtrate and washings were concentrated under reduced pressure. The glassy residue of α-tocopherol succinyl dodecaethylene glycol (cpd 13) was dried in a dessicator under vacuum (oil pump) for 2 h. Yield: 300.6 mg (0.28 mmol; 82%). Diol hexane-iPrOH 6/4, R_f = 0.25 (tailing). ^{1}H NMR ($CDCl_3$) δ 0.85 (d, J = 6.6 Hz, 6H, 4eMe and 8eMe), 0.87 (d, J = 6.6 Hz, 6H, H13e + 12eMe), 1.00–1.10 (m, 2H, H3e), 1.12–1.16 (m, 2H, H11e), 1.23 (s, 3H, 2dMe), 1.20–1.30 (m, 6H, H5e + H7e + H9e), 1.35–1.45 (m, 2H, H4e + H8e), 1.53 (m, 1H, H12e), 1.77 (m, 2H, H3d), 1.97 (s, 3H, 5dMe), 2.01 (s, 3H, 7dMe), 2.08 (s, 3H, 8dMe), 2.58 (brt, J = 6.7 Hz, 2H, H4d), 2.79 (brt, J = 6.9 Hz, 2H, H3c), 2.93 (m, 2H, H2c), 3.59–3.73 (m, 46H, H2b–24b), 4.27 (m, 2H, H1b). ^{13}C NMR ($CDCl_3$) δ 11.80 (8dMe), 12.08 (5dMe), 12.93 (7dMe), 19.65 (8eMe^a), 19.75 (4eMe^a), 20.57 (C4d), 21.00 (C2e), 22.63 (C13e^b), 22.72 (12eMe^b), 23.54–24.23 (br signal, 2dMe), 24.42 (C6e), 24.78 (C10e), 27.96 (C12e), 28.81 (C2c), 29.07 (C3c), 31.06 (br signal, C3d), 32.68 (C4e^c), 32.77 (C8e^c), 37.26, 37.40 and 37.42 (C3e + C5e + C7e + C9e), 39.35 (C11e), 39.49–40.48 (br signal, C1e), 61.67 (C12b), 63.91 (C1b), 69.04 (C2b), 70.26, 70.50, 70.54, 70.59 and 72.62 (C3b to C23b), 75.02 (C2d), 117.34 (C10d), 122.98 (C7d), 124.93 (C5d), 126.63 (C8d), 140.42 (C6d), 149.39 (C9d), 170.93 (C1c), 172.19 (C4c). Analysis: calcd. for $C_{57}H_{102}O_{17}$ $0.8CH_2Cl_2$: C, 61.58; H, 9.26. Found: C, 61.73; H, 9.29.

2.3. Physicochemical characterization

Cryo-TEM: the method [19] involved a home-made guillotine for sample freezing. A droplet of 3 μL sample dispersion was deposited onto a copper grid covered with a perforated carbon film containing holes of about 2 μm in diameter. A filter paper was pressed on the liquid side of the grid (blotting) for removing excess sample solution. Immediately after liquid removal, the grid, held by tweezers, was propelled into liquid ethane. For obtaining micelle images, a home-built environmental chamber similar to the one described by Egelhaaf et al. [20] was used. The humidity was set to 100% and temperature to 23 °C. After the samples were vitrified, frozen grids were stored in liquid nitrogen and

transferred into a cryo-holder kept at −180 °C. Sample analysis was performed in a Philips CM12 TEM at a voltage of 80 kV. Low dose procedures were applied to minimize beam damage.

NMR self-diffusion: all experiments were performed on a Bruker DSX-400 NMR spectrometer (^{1}H Larmor frequency 400.13 MHz) at 25 °C. For the diffusion experiments, a Bruker DIFF25 diffusion probe was used modified with a home-built RF-coil (courtesy of Dr. Magnus Nydén). The 90° proton pulse width was 10 μs. The temperature was set to 25 °C and controlled by the cooling water that passed through the gradient coils. A stimulated echo pulsed field gradient pulse sequence was used. Experimental diffusion data was analyzed using various software; the CORE program, the Bruker software XWINNMR v3.0 and v3.5, and in-house software based on the python programming language that allowed estimation of errors in the fitting parameters.

2.4. Bioavailability studies

Tissue culture: Caco-2 HTB37 cells were cultured in Dulbecco's modified Eagle's medium containing 4.5 g glucose/L, 20% foetal bovine serum, 1% non-essential amino acids, 150 μg/mL gentamicin, 1 μg/mL fungizon, penicillin 100 U/mL and streptomycin 100 mg/mL in a humidified incubator of 10% CO_2, 90% air at 37 °C.

Mixed micelle preparation: into a dark Pyrex tube, previously washed with acetone, 26 μM (cpd 9) or (cpd 13) was mixed with 100 μM monoolein, 50 μM lysophosphatidylcholine, 33 μM oleic acid, and 2 mM taurocholic acid (all final concentrations). The solvents were evaporated under a stream of nitrogen gas for 90 min at room temperature. 15 mL of tissue culture medium were added to every preparation and vigorously vortex mixed for 2 min in order to obtain the mixed micelles solutions of compounds (cpd 9) or (cpd 13). Additionally, in order to see the effect of the self-assembly structure on the absorption, 26 μM solutions of one or the other of the pure compounds in tissue culture medium were prepared. The solutions were sonicated to dissolve the compounds. Mixed micelles solutions and preparations with the pure compounds were stored for stability analysis at room temperature (between 20 and 25 °C), 10% CO_2 90% air 37 °C for 24 and 48 h. The samples were stored at −20 °C until analysis.

Uptake experiment with Caco-2 HTB37 monolayers: Caco-2 HTB37 cells were seeded at a density of 5×10^5 cells/well on PET membrane (0.4 μm pore size) inserts (Falcon, Milian, Geneva, Switzerland) and cultured for 21 d. The medium was changed every second day. For absorption experiments, compounds (cpd 9) and (cpd 13) were loaded into the apical side of the cells either as mixed micelles or in their pure form in tissue culture medium. After an incubation period of 24 h, the medium at the apical and basolateral sides was collected and stored at −20 °C pending analysis. Cells were lyzed with 5% sodium dodecyl sulfate and the lysate collected and stored at −80 °C. For tocopherol and tocopherol succinate analysis and quantification, the lyzed cells were sonicated for 20 s on ice and then transferred into dark Pyrex tubes. The Eppendorf tubes that contained the cell lysates were washed with 500 μL ethanol and vortex mixed for 15 s, then ethanol was added to the Pyrex tube containing the lysate. 10 μL Butyl hydroxytoluene (EtOH 35 mg/100 mL) and 3 mL hexane were added and the tubes vortex mixed for 15 s. The tubes were centrifuged at 1272 g for 5 min at 4 °C. The organic phase was transferred to a clean tube and evaporated under a stream of nitrogen gas. The hexane extraction step was repeated. After complete evaporation of the solvent, the residual material was reconstituted in 200 μL acetonitrile and vortex mixed for 15 s. This solution was analyzed by reversed-phase HPLC with MS. For the analysis of start solution, apical and basolateral media, the same hexane extraction procedure was used after adding 500 μL of ethanol to 0.75 mL of medium.

Lyzed cells were sonicated for 20 s on ice, 3 vol of acetone (2.7 mL) were added and the samples were vortexed and centrifuged for 10 min at 4 °C at maximum speed on a table top centrifuge. The supernatant was collected into a dark Pyrex tube and evaporated under a stream of nitrogen gas. After complete evaporation of the solvent, the residual material was reconstituted in 1 mL water and diluted five-fold before analysis. The same protocol was followed for the apical and basolateral media where 0.75 mL of medium was precipitated with 2.25 mL of acetone.

Protein assay: cell lysates were also used for protein concentration measurements using the bicinchoninic acid Protein Assay Kit (Thermo Fisher Scientific, Lausanne, Switzerland). Cell lysates were diluted 10-fold in water. Into a 96 well plate, 10 μL of each sample was loaded and 200 μL of reagent mix added (50× reagent A and 1× reagent B as suggested by the manufacturer). The plate was incubated for 30 min at 37 °C and read at 590 nm. Bovine serum albumin was used to establish a standard curve from 0.0325 to 2 mg/mL.

HPLC of compounds (cpd 9) and (cpd 13): analysis after HPLC was performed on-line by a mass spectrometry detector system (Agilent Technology Inc., Urdorf, Switzerland) equipped with an APCI source. The mobile phases were methanol and acetonitrile/water at 80:20 (v/v) acidified with formic acid (0.1%), using a C18 column (YMC-Pack Pro, 250 mm × 4.6 mm, Europe, GmbH). Injection volume was 2 μL, runtime 25 min and the flow rate 1.2 mL/min isocratically. Detection was using APCI in positive mode. For analysis with MS, the gas and vaporizer temperatures were set to 350 °C. Drying gas flow was 5.0 mL/min, nebuliser pressure 60 psig, capillary voltage 3000 V, corona current 4 μA, fragmentor 200 V, gain 1.0 EMV and dwell time 139 s. Quantification was made at SIM 812 for (cpd 9) and 1076.5 for (cpd 13).

HPLC of (cpd 1) and (cpd 2): the analysis of samples was performed by LC using a Merck Hitachi LaChrom system with a UV detector (Merck, Geneva, Switzerland). The mobile phase was acetonitrile/tetrahydrofuran/methanol/ammonium acetate 1% (533.52/193.60/53.72/28, w/w). The column was a Nova-Pak 3.9 mm × 300 mm, 4 μm C18 column (YMC-Pack Pro, 250 mm × 4.6 mm). The injection volume was 100 μL and the flow rate was 1.5 mL/min for the Nova-Pak and 1.3 for the YMC column. Analysis was for 20 min at room temperature. Compounds (cpd 1) and (cpd 2) were quantified at 297 nm or 280 nm and with a fluorimeter set with Ex. 298 nm, Em. 328 nm.

Cell metabolism of tocopherol derivatives: in order to get sufficiently relevant statistical data from the bioavailability experiments, cells were cultured for four consecutive weeks. Each week, all formulations were tested in duplicate, giving a total of 8 replicates per formulation. The formulations containing (cpd 13) however, were only added to cell cultures for two weeks, giving a total of four replicates. The solution at the apical side was collected and split into two equal parts. One half was analyzed for the non-absorbed (cpd 9) or (cpd 13) and the other half was used to extract and analyze (cpd 1) and (cpd 2). The basolateral solution was treated in the same way. The cells were lyzed and the lysates collected. One replicate was used to extract (cpd 1) and (cpd 2), while the other was used to analyze (cpd 9) and (cpd 13) that had been taken up by the cells.

Starting formulation: all formulations were made up to a final concentration of 26 μM tocopherol equivalents, equal to 39 nmol total per experiment. All concentrations for the analysis were calculated on the quantity found by adding all compartments (i.e. 39 nmol would be recovered in the three compartments after the absorption studies if there was 100% recovery). In the empty mixed micelles, the amounts of (cpd 1) and (cpd 2) observed were between 0 and 0.05 nmol, which most likely arises from the presence of trace amounts of (cpd 1) in the tissue culture medium. This amount is low compared to the formulations where

tocopherol derivatives were present and was therefore ignored in the absorption experiments.

Incorporation of (cpd 1) and (cpd 2) was observed in the starting solutions (5.1% and 66%, respectively). A small amount (3.8%) of (cpd 1) was present in the sample of (cpd 2). The incorporation of (cpd 9) and (cpd 13) into mixed micelles was assumed to be 100% as these compounds can be solubilised in the aqueous phase.

2.5. Molecular calculations for molecular docking

Molecular docking calculations were performed using the GOLD v2.1.2 program (Cambridge Crystallographic Data Centre) using standard protocols.

3. Results

3.1. Synthesis

The preparation of α-tocopherol hexaethylene glycol succinate (cpd 9) was carried out according to Scheme 1. Being a symmetrical compound, hexaethylene glycol bears two equivalent hydroxyl groups. Therefore the key step of the synthesis was the preparation of mono protected hexaethylene glycol (cpd 7). Hexaethylene glycol monobenzyl ether (cpd 7) is a known compound [14–18]. Indeed, (cpd 7) has been prepared previously in 70% yield from two triethylene glycol units [18]. Alternatively, (cpd 7) was directly obtained by benzylation of hexaethylene glycol, under the catalysis of Ag_2O [17] potassium tert-butoxide [14,16], or of sodium hydroxide [15]. In the latter case, the reaction was performed in the presence of an excess of hexaethylene glycol, in order to avoid the formation of hexaethylene glycol dibenzyl ether. In the course of this study, we used an adaptation of the latter method. Thus benzyl bromide (cpd 6) was reacted with four equivalents of hexaethylene glycol (cpd 5), to give the monobenzyl ether (cpd 7) in 72% yield. Compound (cpd 7) was subsequently esterified with α-tocopherol succinate, catalyzed by EDCI, to give the new conjugate (cpd 8) in quantitative yield. Finally the removal of the benzyl protective group by catalytic hydrogenation yielded α-tocopherol hexaethylene glycol succinate (cpd 9) in 91% yield, and we obtained (cpd 9) in a 65.5% overall yield from hexaethylene glycol (cpd 1). This is significantly better than a previous approach [21], based on the direct esterification of (cpd 1) with α-tocopherol succinic acid, which resulted in the formation of (cpd 9) in only 13.3% yield. The structures of all compounds were deduced from the analyses of their ^1H and ^{13}C NMR spectra. Signal assignment was performed with the help of direct, and long distance proton–carbon correlation experiments. Furthermore, in (cpd 8) and (cpd 9), the assignment of the signals of the α-tocopherol succinate moiety were attributed after analysis of published NMR data for α-tocopherol [22,23], and its succinate ester [24]. Based on the analysis of their long distance proton–carbon correlation spectra, however, in the ^{13}C NMR spectra of (cpd 8) and (cpd 9), we have reversed the assignments of the C5d and C7d signals, as compared to previous data [24]. In the ^{13}C NMR spectrum of (cpd 8), esterification of position 1b of the hexaethylene glycol chain is illustrated by the downfield shift of C1b (2.3 ppm) and the upfield shift of C2b (1.2 ppm), as compared to the ^{13}C NMR spectrum of hexaethylene glycol monobenzyl ether (cpd 7). On the other hand, the removal of the benzyl group in (cpd 9) was accompanied by an upfield shift for C12b (7.7 ppm), as compared to the ^{13}C NMR spectrum of (cpd 8).

The preparation of α-tocopherol dodecaethylene glycol succinate (cpd 13) was dictated by the availability of dodecaethylene glycol monobenzyl ether (cpd 11). Dodecaethylene glycol is commercially available, although at fairly high cost. Therefore we considered it more advantageous to prepare directly dodecaethylene glycol monobenzyl ether (cpd 11) from hexaethylene glycol monobenzyl ether (cpd 7) (Scheme 2). This first involved the activation of the free alcohol of (cpd 7) in the form of its tosylate ester (cpd 10). (Cpd 10) has been previously prepared by tosylation (*p*-toluenesulfonyl chloride) of hexaethylene glycol monobenzyl ether in pyridine [15], or under the catalysis of Ag_2O [17]. In the present work, we have adopted a slightly modified procedure using triethylamine as a base. Finally a "Williamson condensation" of (cpd 10) with an excess of hexaethylene glycol (cpd 5) yielded the new dodecaethylene glycol monobenzyl ether (cpd 11). Finally the preparation of α-tocopherol dodecaethylene glycol succinate (cpd 13) from (cpd 11), followed a similar procedure as for the preparation of (cpd 9) (Scheme 3). Both (cpd 12) and (cpd 13) have not been synthesized as pure compounds before.

If (cpd 9) or (cpd 13) contained free α-tocopherol (cpd 1) and α-tocopherol succinate (cpd 2), this could have an effect on both the self-assembly structure (equivalent to introduction of an oil) and the bioavailability experiments. Hence it was important to carefully analyze the purity of the compounds. Thin layer chromatography, ^1H and ^{13}C NMR analyses, and elemental analyses of compounds (cpd 9) and (cpd 13) confirmed the absence of (cpd 1) and (cpd 2). No change in purity (NMR and HPLC spectra) was observed after storage for 15 months at -20 °C. From full scan HPLC and ^1H NMR, no free polyethylene glycol was detected. (Cpd 9) and (cpd 13) were also analyzed for their stability in water. NMR self-diffusion experiments were performed on fresh samples and on samples stored for two weeks at 22 °C, and showed no tendency of structural or compositional change. HPLC–MS analyses were performed on the freshly solubilised compounds in cell culture medium (DMEM) and on the compounds after incubation under the conditions for the cell absorption studies (22 °C for 24 h and at 10% CO_2 90% air 37 °C for 24 h). No indication of hydrolysis or change of sample composition was observed.

3.2. Physicochemical characterization of the compounds

Ultrasound was needed to solubilise 10 mM solutions of (cpd 9) and (cpd 13) in water. Fig. 2 shows the images of the samples obtained from cryo-TEM analysis: for (cpd 9), the formation of vesicles is observed, but the more hydrophilic (cpd 13) forms long rod-like micelles. This shows that the length of the polyethylene glycol chain is responsible for the formation of the different structures. (Cpd 9), with a short hydrophilic chain, will pack in bilayers and form vesicles. (Cpd 13) has a hydrophilic chain length twice the size of (cpd 9) and will, due to steric interactions between the polyethylene glycol chains, pack in rod-like structures.

In order to confirm the results obtained by the cryo-TEM analysis, and that the samples did not induce an artefact in the self-assembly structure, the samples were further investigated by NMR self-diffusion. As a function of observation time, the diffusion experiments for (cpd 9) could be fitted with a constant self-diffusion coefficient and constant parameter to model a distribution of sizes using the CORE program [25]. The average self-diffusion coefficient was 7.1×10^{-12} m^2/s, with a distribution parameter of 0.87 which corresponds to a small dispersity. Using the Stokes–Einstein relationship, a radius of 37 nm can be calculated. Even at these high concentrations, the obstruction factor is negligible. This value is in good agreement with the cryo-TEM images above. When the same CORE protocol was used to fit diffusion experiments on (cpd 13), non-sensible (i.e. impossible) physical results were obtained clearly showing that the vesicle model is incorrect. The diffusion data showed evidence of bi-exponential decay. As a function of observation time, the percentage of each component was constant but one of the two self-diffusion coefficients in the fit became smaller. The data is

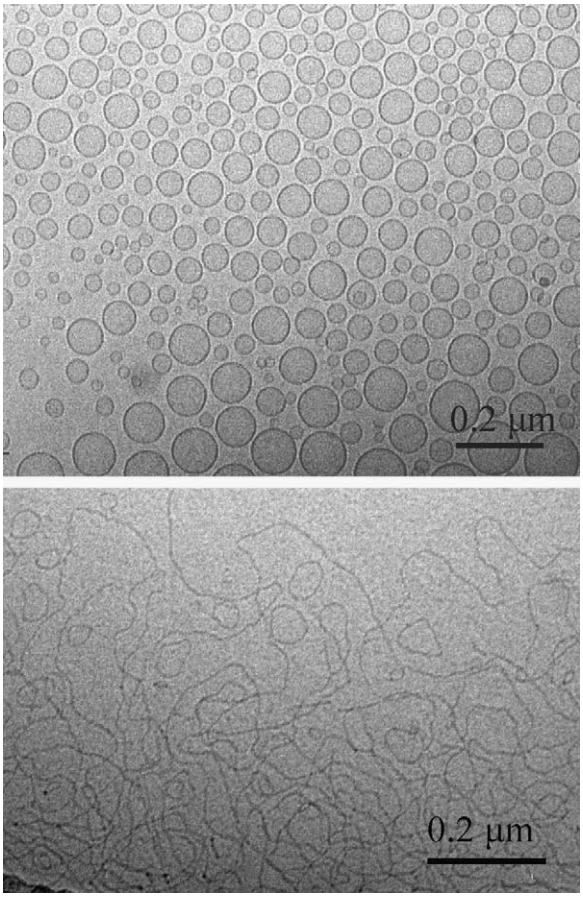

Fig. 2. Cryo-TEM image of (a) vesicles formed by 10 mM (cpd 9), (b) rod-like micelles formed by 10 mM (cpd 13) in pure water.

shown in Fig. 3. Angelico et al. have observed something similar for a system of giant worm-like micelles [26]. They attributed the changing self-diffusion coefficient as a function of observation time to diffusion of the molecules along the worm-like micelle chains. Given the cryo-TEM results, the diffusion data would appear to suggest this structure is the dominant one.

We have measured the self-diffusion properties of the two systems close to the concentrations used in the Caco-2 cell studies in order to relate the bioavailability studies to the physical structure. The experiments on (cpd 9) were performed over the concentration range of 50–200 μM and an observation time from 20 to 200 ms. Given the signal to noise ratio of the experiments at these lower concentrations, the data was fitted to a single exponential function. Over the concentration range and observation time, the values obtained were essentially constant giving a self-diffusion coefficient of $1 \times 10^{-11} \pm 3 \times 10^{-12}$ m^2/s. This value gives a Stokes–Einstein radius of 20 nm. This value is too large to be simple spherical micelles, and suggests that the aggregates remain vesicles upon dilution.

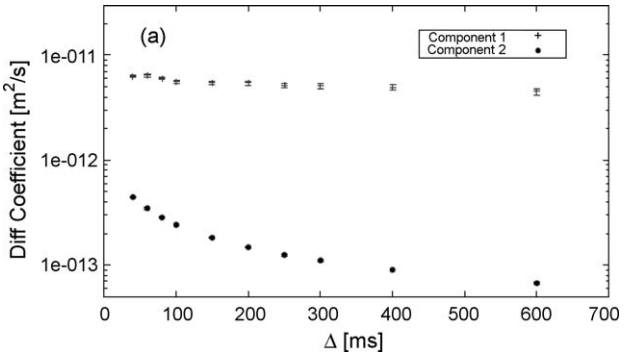

Fig. 3. Self-diffusion coefficients obtained for (cpd 13) at 10 mM as a function of observation time, Δ, using a bi-exponential fit.

3.3. Uptake and metabolism by Caco-2 cells

The hydrolysis and uptake by Caco-2 cells, which are an in vitro model of the enterocytes of the small intestine, of (cpd 1), (cpd 2), (cpd 9) and (cpd 13) was analyzed. Compounds were loaded at the apical side, and passage into the cells, across the cells, and efflux of possible metabolites back to the apical side was measured. Both (cpd 9) and (cpd 13) were incubated either in their pure form (shown above to form vesicles or rod-like micelles) or incorporated into mixed micelles (using bile salts, monoglycerides and fatty acids). Mixed micelles containing tocopherol (cpd 1) or tocopherol succinate (cpd 2), as well as empty mixed micelles, were incubated as controls. The reaction pathways, showing the compounds and metabolites analyzed in the various phases, is shown in Fig. 4, and the results are presented divided into the apical, the intracellular and the basolateral compartments.

For all formulations of (cpd 9) and (cpd 13), both vesicles and the mixed micelles, about 30–50% remained unmetabolised on the apical side after the incubation. There was a slight increase in the amount of (cpd 1) (<0.1 μM) on the apical side as compared to the starting material. In addition, concentration of (cpd 2) on the apical side increased significantly. For (cpd 13), the amounts of (cpd 2) at the apical side after incubation were higher as compared to (cpd 9) (~1.7 μM cf ~0.6 μM), and this relationship applied to all self-assembly structures. Only a very small amount of (cpd 2) was metabolized to (cpd 1) at the apical side (final [(cpd 1)] ~0.6 μM). These results indicate that there is significant but limited apical hydrolysis of (cpd 9) or (cpd 13) into (cpd 2), but very little further metabolism of (cpd 2) into (cpd 1), demonstrating that these Caco-2 cells possess a brush border esterase able to hydrolyze (cpd 9) or (cpd 13) into (cpd 2). The amount of (cpd 2) for both formulations on the apical side is higher than in the cells, but for (cpd 1), the opposite is observed. The amount of (cpd 1) in the cells is higher than in the apical solution, probably indicating that the hydrolysis by the enzyme is the rate-limiting step.

Fig. 5 shows the uptake of (cpd 1) and (cpd 2) by Caco-2 cells. The total amount of (cpd 1) and (cpd 2) taken up by the cells is

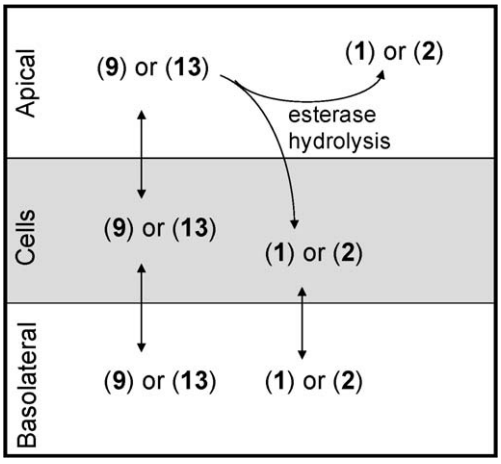

Fig. 4. Schematic illustration of (cpd 9) or (cpd 13) added to the apical side of the Caco-2 cells and the possible hydrolysis and absorption routes of the compound and its derivatives. Compounds ((cpd 1), (cpd 2), (cpd 9) and (cpd 13)) in all compartments (apical, cells, basolateral) were analyzed.

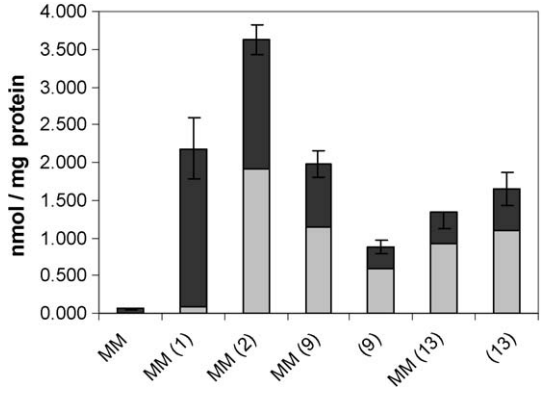

Fig. 5. Presence of (cpd 1) (dark bars) and (cpd 2) (light grey bars) in Caco-2 cells after treatment with compounds shown on the *x*-axis. The error bars show the 95% confidence interval of the mean (±2 SEM (standard error of mean)). Values are normalized to Caco-2 protein content; MM, mixed micellar form.

highest when (cpd 2) is added as mixed micelles, where about half was hydrolyzed and present inside the cells as (cpd 1). Fig. 6 shows the uptake of intact (cpd 9) and (cpd 13). A slightly higher amount of the smaller (cpd 9) is taken up into the cells as compared to (cpd 13). This difference may be caused by the higher molecular weight where diffusion would be the rate-limiting step. (Cpd 4) was also found inside the cells in an intact form [27] but no polyethylene glycol chain length differences were studied. A proportion of (cpd 9) and (cpd 13) taken up into the cells was metabolized into (cpd 1) and (cpd 2) (Fig. 5). For the formulations containing (cpd 9), the cell content of (cpd 1) is somewhat larger than (cpd 2), while for (cpd 13), the opposite is observed. This indicates that there is an active esterase which converts both (cpd 9) and (cpd 13) to (cpd 1) and (cpd 2). However, it exhibits a different specificity for (cpd 9), (cpd 13) and (cpd 2), since the intracellular tocopherol succinate/tocopherol ratio is higher when (cpd 13) is substrate. This is consistent with the modelling studies of the intracellular esterase (see below, Section 3.4). The self-assembly structure also has a major influence on the uptake and metabolism. The total hydrolysis and uptake from (cpd 9) in vesicular form is two-fold lower than in the form of mixed micelles. On the other hand, (cpd 13) in the rod-like form gave a slight increase in total uptake of (cpd 1) and (cpd 2) as compared to the mixed micelles. These findings indicate that the self-assembly structure affects both the cellular uptake and the enzymatic hydrolysis of the tocopherol derivatives. For all experiments, no (cpd 1) or its derivatives were detected in the basolateral compartment, showing that insignificant amounts of (cpd 1) or its derivatives are transported out of the cells to the basolateral side in this model.

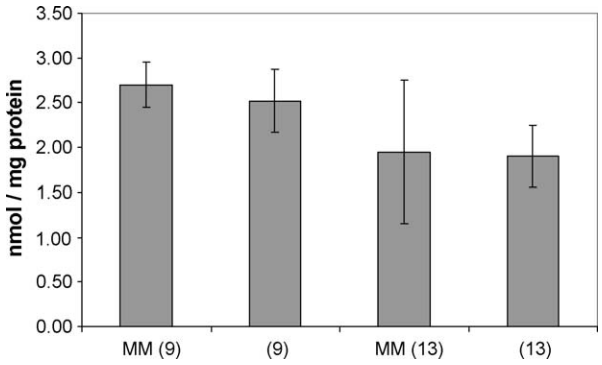

Fig. 6. Uptake of intact (cpd 9) and (cpd 13) by Caco-2 cells. The error bars show the 95% confidence interval of the mean (±2 SEM). Data are normalized to Caco-2 cell protein content; MM, mixed micellar form.

The Niemann-pick C1-like 1 (NPC1L1) protein mediates tocopherol transport into the cell [28] but it is not known if this transporter can also accept tocopherol esters. TPGS may block P-glycoprotein [29], which is an important apical transporter for effluxing compounds back into the gut lumen. Hence the distribution of tocopherol and esters in the Caco-2 cells will depend on the distribution of these transporters, but most importantly on the ability of the carboxyl esterase to release free tocopherol from its esters.

3.4. Molecular docking model for enzyme binding and hydrolysis of tocopherol derivatives

From the results above, it is clear that hydrolysis of the tocopherol derivatives is mediated by the Caco-2 cells. The human carboxyl esterase 1 enzyme, hCE1, contains 523 amino acids and is the major intracellular esterase in Caco-2 cells [30]. hCE1 (EC 3.1.1.1) is a broad-spectrum serine hydrolase, expressed in the liver and in the intestine, and is able to cleave ester, amide and thioester linkages in a wide variety of chemically distinct compounds. The crystal structure of the enzyme [31] reveals that the catalytic domain contains the serine hydrolase catalytic triad (Ser221, Glu354 and His468) at the base of the active site. The substrate-binding gorge contains a large flexible pocket (Leu255, Leu304, Leu318, Leu363, Leu388, Thr252, Met364, Met425, Phe426) on one side of Ser221 and a small rigid pocket (Gly142, Gly143, Leu96, Leu97, Leu100, Leu358, Phe101) on the opposite side (Fig. 7).

For this study, since the result of the hydrolytic reaction is the cleavage of an ester bond, we selected the structure of hCE1 that is co-crystallized with a compound that contains an ester group (PDB entry: 1mx5), a 3D structure of the hCE1 enzyme in complex with the cocaine analogue hematropine. The hydrolytic mechanism has been determined, and is a typical serine protease mechanism characterized by a catalytic triad of Ser221, Glu354 and His468,

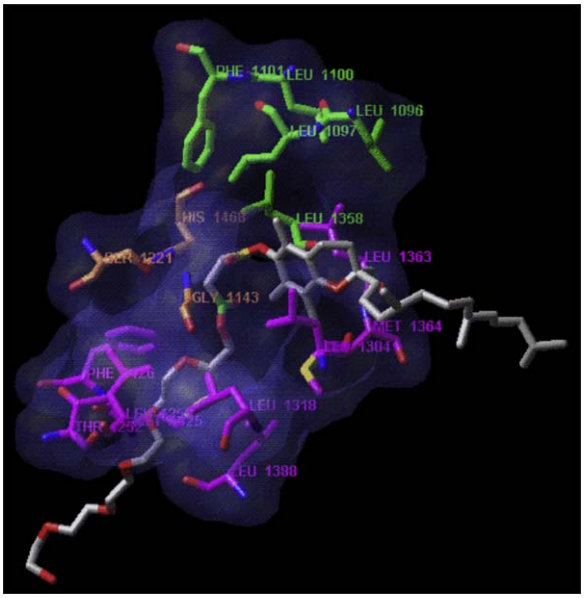

Fig. 7. Representation of the human carboxyl esterase 1 binding gorge. The catalytic triad, the large flexible pocket and the small rigid pocket are displayed in orange, purple and green, respectively. Amino acids are shown as follows: Leu96 as Leu196, Le363 as Leu1363, etc. (Cpd 9) is docked within the active site of the enzyme.

forming a charge-transfer relay network. As the serine oxygen attacks the carboxyl carbon of an ester bond, the hydrogen-bonded histidine functions as a general base to abstract the serine proton while the negatively charged glutamate stabilizes the positive charge that is formed on the histidine residue. This prevents the development of a very unstable positive charge on the serine hydroxyl and increases its nucleophilicity. The hydrolytic mechanism starts with the nucleophilic attack of the ester bond by Ser211 resulting in the formation of a covalent transition state that is stabilized via the amide nitrogen atoms of Gly142 and Gly143. The presence of a water molecule leads to the cleavage of the ester bond. A molecular surface representing the lipophilicity of the enzyme was designed. The entrance of the substrate-binding gorge forms a highly hydrophobic pocket that can fix the tocopherol fragment within the enzyme (Fig. 7). The succinate fragment that contains the two ester linkages fits in the catalytic triad region where they can undergo a nucleophilic attack by the serine oxygen. According to the crystallographic structure of the enzyme and the description of the hydrolytic mechanism with the R-cocaine substrate, the ester linkage is placed within Ser221 and Gly143 residues.

The hCE1 binding site that has been defined in our calculations constitutes the residues that are present in a sphere of 10 Å around the hematropine ligand that was co-crystallized with the enzyme. A reference dataset of molecules was compiled with 20 tocopherol polyethylene glycol succinate derivatives. The polyethylene glycol chain length, *n*, varied from 1 to 20 (i.e. including (cpd 9) and (cpd 13) where *n* = 6 and 12, respectively). Each tocopherol derivative underwent a minimization in order to optimize bond lengths and to relax the possible internal strengths. For each molecule, the software (GOLD v2.1.2) generated 30 solutions. Each proposed binding mode was manually analyzed, checking that the expected molecular interactions were recovered between them and the residues of the active site. Particularly, we focused on the feasibility of nucleophilic attack by the Ser221 oxygen (OSer211) and stabilization by the interaction with the Gly143 amide nitrogen (NGly143). To achieve this, the distances and orientations between the carboxyl groups of the molecules and the OSer211 and NGly143 were measured (Table 1). The lipophilicity of the different compounds was also calculated as it gives information on the increase of the water-solubility of the tocopherol derivatives according to the hydrophilic polyethylene glycol chain length. The

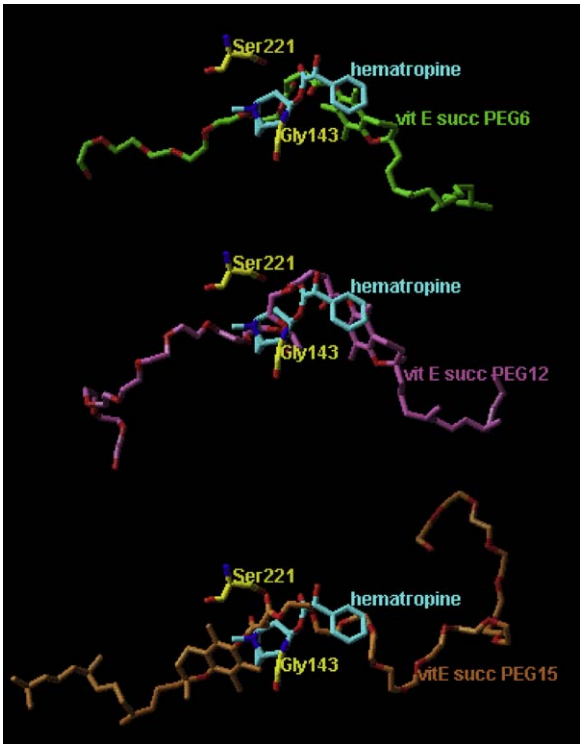

Fig. 8. The three different binding modes that are observed from molecular docking calculations, for *n* = 6 (cpd 9), *n* = 12 (cpd 13) and *n* = 15.

feasibility of the hydrolysis can be deduced by superposing the predicted structures on the hematropine complex determined crystallographically. The distance between OSer211 and the ester linkage carbon on the hematropine is 4.07 Å and the distance between NGly143 and the carboxyl ester oxygen is 5.67 Å.

The first observation that can be made from molecular docking is that there is a linear dependence of the polyethylene glycol length on the hydrolysis of the tocopherol derivatives up to seventeen polyethylene glycol units, beyond which calculations are not feasible. Three different binding modes were observed (Fig. 8). The first binding mode (BM1) places the molecule in such a way that the nucleophile attacks the carboxyl carbon CA (ester

Table 1
Results from the molecular docking calculations. For each tocopherol succinate polyethylene glycol derivative, the feasibility of the nucleophilic attack by Ser211 is evaluated. Distances 1–4 represent the distance between (1) OSer211 and CA (ester carbon between the tocopherol and the succinate fragment), (2) OGly143 and OA (oxygen of the ester bond between the tocopherol and the succinate fragment), (3) OSer211 and CB (ester carbon between the succinate fragment and the polyethylene glycol chain), and (4) OGly143 and OB (oxygen of the ester bond between the succinate group and the polyethylene glycol chain). All distances are given in Å.

Polyethylene glycol chain length	Molecular weight	Log *P*	Distance 1	Distance 2	Distance 3	Distance 4
1	574.4	8.24	6.39	4.20	4.93	5.84
2	618.4	8.05	5.87	4.04	3.54	4.81
3	662.4	7.86	8.28	8.06	5.43	2.81
4	706.4	7.67	4.90	3.90	3.44	5.62
5	750.4	7.48	3.71	5.06	4.61	6.91
6	794.5	7.29	3.12	3.39	4.26	3.05
7	838.5	7.10	4.53	3.63	4.59	4.53
8	882.5	6.91	4.83	5.65	2.86	2.95
9	926.5	6.72	5.83	3.75	2.76	4.79
10	970.5	6.53	6.32	4.59	3.52	5.20
11	1014.6	6.34	3.86	3.10	3.55	5.61
12	1058.6	6.15	5.68	4.99	2.68	5.57
13	1102.6	5.96	9.63	8.20	6.30	6.70
14	1146.6	5.77	5.76	4.57	3.06	3.76
15	1190.6	5.58	4.71	8.97	1.68	4.86
16	1234.7	5.39	5.31	4.52	3.80	6.97
17	1278.7	5.20	4.66	4.28	2.48	4.29

carbon between the tocopherol and the succinate fragment) that leads to the release of (cpd 1). This binding mode is observed by superimposition of the predicted structures for the compounds for which the polyethylene glycol length is equal to 4, 5, 6 (=(cpd 9)), 7, 8 and 11 with the hematropine co-crystallized structure. A second binding mode (BM2) places the molecules with the carboxyl carbon CB (ester carbon between the succinate fragment and the polyethylene glycol chain) aligned for hydrolysis. The two products from the reaction are (cpd 2) and a polyethylene glycol chain. This second binding mode is observed for $n = 9, 10, 12$ (=(cpd 13)), 13 and 14. For binding modes BM1 and BM2, the polyethylene glycol chain is placed within the enzyme-binding gorge, the tocopherol fragment being fixed in the hydrophobic pocket as described above. The third binding mode (BM3), in contrast, places the tocopherol moiety within the binding gorge and the cleavage occurs on the carboxyl carbon CB. This third binding mode is observed for $n = 15$ and 17.

For the molecules with $n = 1$, 3 and 16, the feasibility of hydrolysis was not supported by the molecular docking calculations. In general, therefore, for the shorter polyethylene glycol chains (up to $n = 8$ units, but also $n = 11$), the molecule preferentially enters the active site with the polyethylene glycol chain in the large flexible pocket and the ester between the vitamin and the succinate is attacked, yielding a free tocopherol (cpd 1) molecule. With longer polyethylene glycol chains, steric hindrance plays a role in the active site, the molecule is slightly pushed out of the large flexible pocket and the ester between the succinate and polyethylene glycol becomes the most available, rendering a tocopherol succinate (cpd 2) as the product. For even longer chains, from 15 units, the polyethylene glycol chain does not fit to the flexible pocket due to steric limitations, but instead the tocopherol moiety will fit into the pocket. As this molecule is smaller than the polyethylene glycol chain, it will fit more deeply into the pocket and cleavage will be favoured (cpd 2).

4. Discussion

This study describes the synthesis of two pure and defined α-tocopherol polyethylene glycol succinate esters with polyethylene glycol chain lengths of 6 and 12 ethylene oxide units ((cpd 9) and (cpd 13), respectively, see Fig. 1). The compounds were free from α-tocopherol (cpd 1) and α-tocopherol succinate (cpd 2) and were stable both dry and in solution. At 10 mM, (cpd 9) formed vesicular structures with radii of ca. 37 nm but with a large dispersity in size, whereas (cpd 13) formed rod-like micelles. On dilution to physiological concentrations, the aggregated structures were still present even though the diffusion coefficients were somewhat larger indicating a smaller self-assembly structure. One aim of the study was to estimate the bioavailability of the novel compounds with respect to their molecular and self-assembly structures. It is important to make a distinction between the structure of the aggregate and the molecular effect on hydrolysis and uptake. The structure of the aggregate will mainly influence the total amount of compound taken up, whereas the molecular structure will have an impact on the site of hydrolysis and hence the distribution of products. Our study demonstrates that both size and self-assembly structure markedly affect the hydrolysis and uptake. The highest total uptake was observed for mixed micelles containing (cpd 2), probably since mixed micelles are the smallest of the structures. When both are in the mixed micellar form, twice as much (cpd 2) is taken up by the cells compared to (cpd 1). For the polyethylene glycol derivatives, the highest amount of total (cpd 1) and (cpd 2) absorbed into the cells was observed for the mixed micelles containing (cpd 9) and the rods based on (cpd 13). A difference was observed in the ratio of (cpd 1) to (cpd 2) taken up by the cells. For (cpd 9), the favoured site of hydrolysis is between the tocopherol and the succinate moiety while hydrolysis of (cpd 13) leads to a higher amount of (cpd 2), thus hydrolysis is favoured between the succinate and the polyethylene glycol moieties. These results were supported by the enzymatic docking model where it was found that hydrolysis to (cpd 1) was favoured for derivatives with polyethylene glycol chain lengths up to 8 units while longer chain lengths would favour hydrolysis to (cpd 2). Some (cpd 9) and (cpd 13) were taken up into the cells intact, i.e. without hydrolysis. For (cpd 9), a slightly larger amount was found in the cells compared to (cpd 13), most likely due to the faster diffusion though the cell membrane of the smaller compound.

Acknowledgements

Francia Arce Vera is thanked for recording the ^{1}H and ^{13}C NMR spectra and Isabelle Tavazzi for assisting in the extraction of tocopherol from the cells and analysis. Cédric Zhand is thanked for the HPLC analysis of the tocopherol and tocopherol succinate and Birgit Holst for discussions on the bioavailability of the vitamins. The study was funded in full by the Nestlé Research Center, Lausanne, Switzerland.

References

[1] Azzi A. Molecular mechanism of alpha-tocopherol action. Free Radic Biol Med 2007;43:16–21.
[2] Kushi LH. Vitamin E and heart disease: a case study. Am J Clin Nutr 1999;69:1322S–9.
[3] Traber MG, Frei B, Beckman JS. Vitamin E revisited: do new data validate benefits for chronic disease prevention? Curr Opin Lipidol 2008;19:30–8.
[4] Traber MG, Atkinson J. Vitamin E, antioxidant and nothing more. Free Radic Biol Med 2007;43:4–15.
[5] Massey JB. Interfacial properties of phosphatidylcholine bilayers containing vitamin E derivatives. Chem Phys Lipids 2001;109:157–74.
[6] Traber MG, Schiano TD, Steephen AC, Kayden HJ, Shike M. Efficacy of water-soluble vitamin E in the treatment of vitamin E malabsorption in short-bowel syndrome. Am J Clin Nutr 1994;59:1270–4.
[7] Combs Jr GF. Studies on the utilization of vitamin E alcohol and esters by the chick. Poult Sci 1978;57:223–9.
[8] Takata J, Karube Y, Nagata Y, Matsushima Y. Prodrugs of vitamin E. 1. Preparation and enzymatic hydrolysis of aminoalkanecarboxylic acid esters of D-alpha-tocopherol. J Pharm Sci 1995;84:96–100.
[9] Takata J, Matsunaga K, Karube Y. Delivery systems for antioxidant nutrients. Toxicology 2002;180:183–93.
[10] Vazquez B, Ortiz C, San Roman J, Plasencia MA, Lopez-Bravo A. Hydrophilic polymers derived from vitamin E. J Biomater Appl 2000;15:118–39.
[11] Rosenau T, Habicher WD, Streicher H. Chromanyl-ascorbic acid derivatives, their production and use. Patent, BASF A-G. 96-19633560[19633560]; 1996.
[12] Rosenau T, Habicher WD. "Vitamin CE," a novel prodrug form of vitamin E. Chem Pharm Bull 1997;45:1080–4.
[13] Morisaki K, Ozaki S. Design of novel hybrid vitamin C derivatives: thermal stability and biological activity. Chem Pharm Bull 1996;44:1647–55.
[14] Butterworth JF, Moran JR, Whitesides GM, Strichartz GR. Limited nerve impulse blockade by "leashed" local anesthetics. J Med Chem 1987;30:1295–302.
[15] Selve C, Achilefu S, Mansuy L. A novel procedure for the synthesis of ether-bridged perfluoro non-ionic surfactants. Synth Commun 1990;20:799–807.
[16] Peeters E, Janssen HM, Van Zundert MF, Van Genderen MHP, Meijer EW. The synthesis and polymerization of oxo-crown ethers. Acta Polym 1996;47:485–91.
[17] Loiseau FA, Hii KK, Hill AM. Multigram synthesis of well-defined extended bifunctional polyethylene glycol (PEG) chains. J Org Chem 2004;69:639–47.
[18] Chen B, Baumeister U, Pelzl G, Das MK, Zeng X, Ungar G, et al. Carbohydrate rod conjugates: ternary rod-coil molecules forming complex liquid crystal structures. J Am Chem Soc 2005;127:16578–91.
[19] Adrian M, Dubochet J, Lepault J, McDowall AW. Cryo-electron microscopy of viruses. Nature 1984;308:32–6.
[20] Egelhaaf SU, Schurtenberger P, Muller M. New controlled environment vitrification system for cryo-transmission electron microscopy: design and application to surfactant solutions. J Microsc (Oxford) 2000;200:128–39.
[21] Zhang Y, Gold LC. Preparation of tocopherol-modified pharmaceuticals. Patent, 978222[2005096340]; 2004.
[22] Baker JK, Myers CW. One-dimensional and two-dimensional 1H- and 13C-nuclear magnetic resonance (NMR) analysis of vitamin E raw materials or analytical reference standards. Pharm Res 1991;8:763–70.
[23] Matsuo M, Urano S. Carbon-13 NMR spectra of tocopherols and 2,2-dimethylchromanols. Tetrahedron 1976;32:229–31.

[24] Witkowski S, Wawer I. 13C NMR studies of conformational dynamics in alpha-tocopherol esters in solution and solid state. J Chem Soc Perkin Trans 2002;2:433–6.
[25] Stilbs P. Component separation in NMR imaging and multidimensional spectroscopy through global least-squares analysis, based on prior knowledge. J Magn Reson 1998;135:236–41.
[26] Angelico R, Olsson U, Palazzo G, Ceglie A. Surfactant curvilinear diffusion in giant wormlike micelles. Phys Rev Lett 1998;81:2823–6.
[27] Traber MG, Thellman CA, Rindler MJ, Kayden HJ. Uptake of intact TPGS (D-alpha-tocopheryl polyethylene glycol 1000 succinate) a water-miscible form of vitamin E by human cells in vitro. Am J Clin Nutr 1988;48:605–11.
[28] Narushima K, Takada T, Yamanashi Y, Suzuki H. Niemann-pick C1-like 1 mediates alpha-tocopherol transport. Mol Pharmacol 2008;74:42–9.
[29] Wempe MF, Wright C, Little JL, Lightner JW, Large SE, Caflisch GB, et al. Inhibiting efflux with novel non-ionic surfactants: rational design based on vitamin E TPGS. Int J Pharm 2009;370:93–102.
[30] Imai T, Imoto M, Sakamoto H, Hashimoto M. Identification of esterases expressed in Caco-2 cells and effects of their hydrolyzing activity in predicting human intestinal absorption. Drug Metab Dispos 2005;33:1185–90.
[31] Bencharit S, Morton CL, Xue Y, Potter PM, Redinbo MR. Structural basis of heroin and cocaine metabolism by a promiscuous human drug-processing enzyme. Nat Struct Biol 2003;10:349–56.